

## Communications to the Editor

### Nondestructive Measurement of a Glass Transition Temperature at Spin-Cast Semicrystalline Polymer Surfaces

J. Hyun,<sup>\*,†</sup> D. E. Aspnes, and J. J. Cuomo

Department of Materials Science and Engineering,  
North Carolina State University,  
Raleigh, North Carolina 27695-7907

Received July 21, 2000

Revised Manuscript Received November 1, 2000

Despite the importance of glass-forming materials, the glass transition itself remains poorly understood. Although the glass transition is not a thermodynamic phase transition,<sup>1</sup> derivative thermodynamic quantities such as thermal expansion and volume-dependent properties such as the refractive index show discontinuities as this condition is reached.<sup>2,3</sup> Polymer molecules provide an attractive opportunity for studying this transition since all polymers show characteristic properties of a brittle solid or glass at temperatures below a certain level and become flexible above, where major segments of the polymer chains achieve some degree of translational freedom.<sup>4</sup> Moreover, polymers can be easily cast onto any substrate from solution.

In particular, poly(ethylene terephthalate) (PET) is a semicrystalline polymer composed of crystallites embedded in an amorphous polymer matrix, and it exhibits strong optical absorption in the ultraviolet.<sup>5</sup> This allows us to tailor the penetration depth of light with wavelength, which in turn allows us the opportunity to investigate the glass transition in both bulk and surface regions of the same sample by examining the optical properties at both short and long wavelengths. Here, we use ellipsometry to monitor these transitions.

**Experiment.** PET (Aldrich,  $M_v = 18\,000$ ) dissolved in *o*-chlorophenol was cast onto a silicon wafer that

previously had been cleaned ultrasonically for 10 min in acetone. For reproducibility, all samples were annealed above the bulk glass transition temperature  $T_g$  by ramping their temperature at 50 °C/min to 80 °C and then maintaining it at 80 °C for 5 min. Following this, process data were obtained as a function of temperature using a rotating-analyzer spectroscopic ellipsometer with a spectral range of 1.5–6.0 eV. The ellipsometer was a rotating-analyzer system with a spectral range from 1.5 to 6.0 eV and operates at an angle of incidence of 67.08° as described elsewhere.<sup>6</sup> For the measurement the samples were first again heated to 80 °C and then cooled in stages with data taken at various temperatures as indicated in the figures. Temperature was regulated to within  $\pm 0.5$  °C by a controller. Each temperature was held for 2 min before proceeding to the next. During the constant-temperature interval, ellipsometric data were taken at preselected wavelengths. Each point shown in the subsequent figures represents averaging over 250 optical cycles (approximately 2.5 s per data point). The radio-frequency (rf) plasma system uses inductively coupled equipment and operates at 13.54 MHz. Specimens were mounted on the flat sample holder, and the chamber was evacuated to a base pressure of  $10^{-6}$  Torr or better. Treatment was performed at an operating pressure of  $5 \times 10^{-4}$  Torr for 30 s and at an rf power of 50 W while introducing only oxygen gas.

**Results.** The ellipsometrically determined dielectric function of PET is shown in Figure 1. These data were obtained for a 500 nm thick PET film on a Si substrate and were obtained by reducing the original ( $\tan \psi$ ,  $\cos \Delta$ ) ellipsometric data within the three-phase (substrate/overlayer/ambient) model. What constitutes a surface from the perspective of one technique can be the bulk from the perspective of another or also under different conditions with the same technique. As can be seen, PET is transparent below 4 eV, but from 4.8 to 6.0 eV the penetration depth of light is of the order of 100 nm. This allows both bulk and near-surface properties to be measured by changing the wavelength. At the short-

\* To whom correspondence should be addressed.

† Current address: Department of Biomedical Engineering, Duke University, Durham, NC 27708-0281.

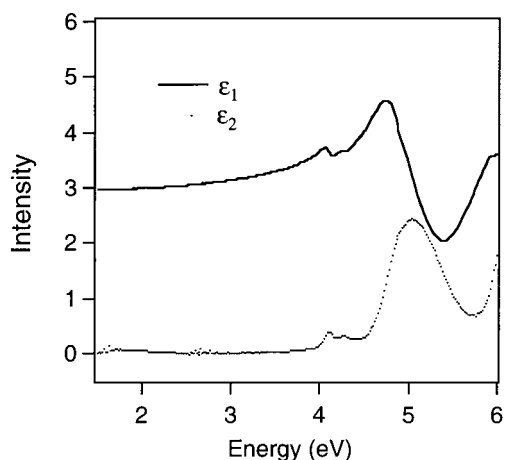


**Figure 1.** Dielectric function of poly(ethylene terephthalate) from 1.5 to 6.0 eV.

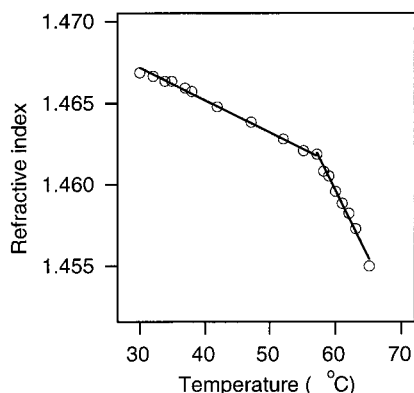


**Figure 2.** Dependence of the refractive index on temperature at 5.8 eV.

wavelength end penetration depths at 5.5 and 5.8 eV are 25 and 15 nm, respectively.

Figure 2 shows the temperature dependence of the refractive index  $n$  determined at 5.8 eV from ellipsometric data. These data clearly exhibit two distinct regions highlighted by the line segments. By effective-medium theory<sup>7</sup> the refractive index is related to the density of the material, and hence the intersection of the two straight-line segments represents a discontinuity in the rate at which the density changes with temperature, i.e., in the thermal expansion coefficient. It is known that the expansion coefficient of a polymer is significantly higher above the glass transition temperature than in the glassy state. This allows us to assign the temperature at which the slope discontinuity occurs to the glass transition temperature  $T_g$ . Because the penetration depth of light here is below 30 nm, we consider this to be the glass transition temperature of the surface. To ensure that the incident beam was not affecting the data, we examined the response with the sample at 90 °C for 15 min. No change was observed, as expected for a beam with an incident intensity of the order of nW/cm<sup>2</sup>. It is therefore clear that the observed discontinuity does not arise from the scission or breakage of chemical bonds, but from the change of free volume between the chains. Similar results are observed for measurements of the refractive index at 1.5 eV, although the break occurs at different temperatures. This is not surprising since at 1.5 eV the penetration depth of the light is large, and the refractive index measured is essentially equal to that of the bulk. The

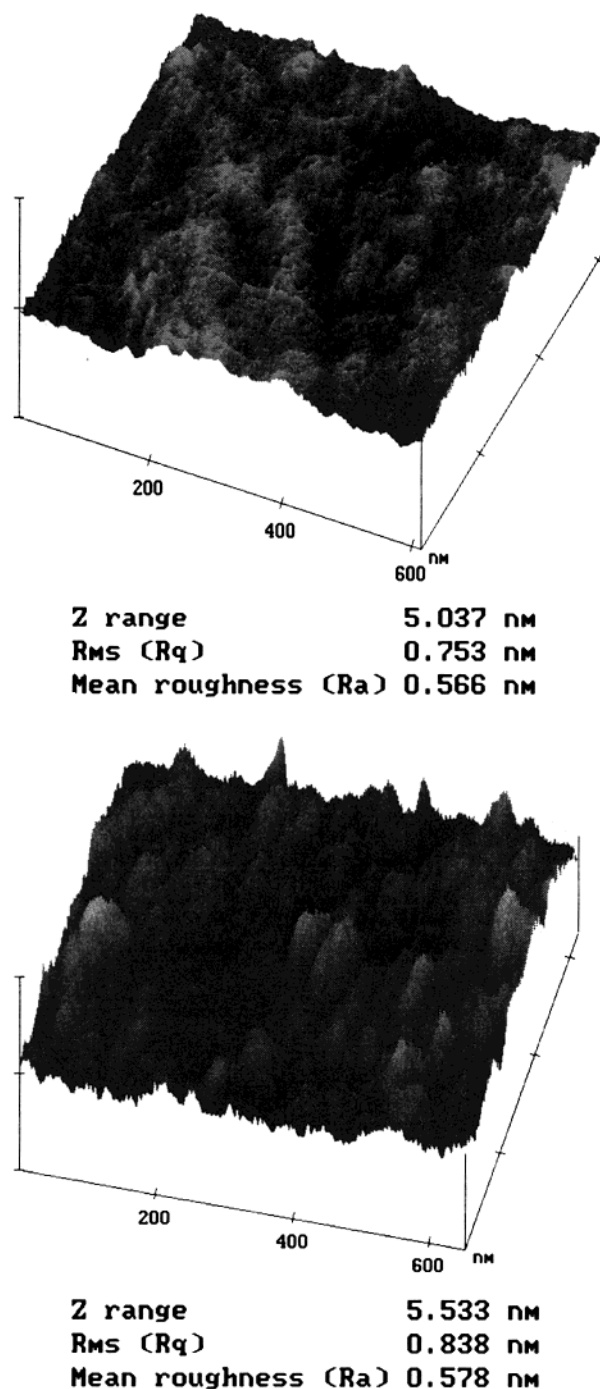


**Figure 3.** AFM images of an untreated (A) and a plasma-treated polymer surface (B).

**Table 1.** Glass Transition Temperature of Poly(ethylene terephthalate) Obtained from  $\Psi$  and  $n$  at Different Photon Energies

photon energy (eV)	untreated		plasma treated	
	$\Psi$	$n$	$\Psi$	$n$
1.5	71	72	65	59
5.5	65	68	56	53
5.8	56	61	53	52

results of the different measurements are summarized in Table 1.

Molecular dynamics simulations of the free surface region of a glassy polymer have been performed by Mansfield and Theodorou.<sup>8</sup> The different regions are characterized by their densities. The local mobility is

simulated within each region. According to these simulations, there is considerable enhancement of atomic mobility in the outermost region compared to the internal regions as a consequence of the decreased surface density and increased free volume. In fact, the surface consists not only of a solid phase but also of transition phases with liquidlike or vaporlike behavior.<sup>9</sup> The existence of a liquidlike layer at the free surface of the film is apparently what reduces  $T_g$ .<sup>3a</sup> In particular, the simulation showed that for several tens of angstroms into the film  $T_g$  was lower by 22 °C than in the bulk, consistent with the results observed here. It is hard to conclude that the enhanced chain mobility is the direct reason for reduced  $T_g$  in this report because of a simplified system not crystalline used for the simulation. However, the density variation and increased free volume at the surface does reduce  $T_g$ .

An oxygen-plasma-treated polymer surface was also characterized. This surface shows considerably different surface properties with respect to the untreated surface. Plasma treatments are expected to create very low molecular weight fragments on the surface,<sup>10</sup> which can be divided into three species: liquidlike molecules, plasticizers, and oligomers. Plasticizers such as dibutyl phthalate and diisooctyl phthalate are relatively small in size compared to polymer molecules and can penetrate into the polymer matrix and establish polar attraction forces between it and the chain segments. These attractive forces reduce the cohesive forces between the polymer chains. This increases segmental mobility, thereby reducing  $T_g$ . These plasticizers also have a chemical structure similar to the phenyl-ring-containing fragments produced in plasma-processed polymers such as PET and polystyrene. These fragments can also diffuse or penetrate into the bulk, increasing the free volume. This change of free volume is expected to reduce  $T_g$  on plasma-treated polymer surfaces.

Table 1 shows the  $T_g$  of PET obtained at photon energies for untreated and oxygen-plasma-treated polymer surfaces. As a cross-check, we determined  $T_g$  from both the variation of the ellipsometric parameter  $\psi$  with  $T$  and the value of  $n$  calculated from  $\psi$  and  $\Delta$ . As expected from the above discussion, the plasma-treated surface shows a lower  $T_g$  than the corresponding untreated surface. In particular, the value at 5.8 eV is

lower than at the other photon energies. The value of  $T_g$  obtained at 1.5 eV can be considered as bulk compared with the values at 5.5 and 5.8 eV. The possible development of a rough surface during plasma treatment was prevented by using an inductively coupled rf system and mild treatment conditions. The AFM images in Figure 3 verify that there is no roughening of the film surface after plasma treatment.

In summary, we report a nondestructive characterization of the surface glass transition temperature in PET by analysis of the variation of the ellipsometrically measured refractive index with temperature, using the spectral dependence of the penetration depth of light to discriminate surface and bulk transitions. The surface  $T_g$  is lower than that of the bulk for spin-cast semicrystalline-PET films because of density variation, and  $T_g$  is lowered further by plasma processing.

## References and Notes

- (1) Gibbs, J. H.; DiMarzio, E. A. *J. Chem. Phys.* **1958**, *28*, 373.
- (2) (a) Keddie, J. L.; Jones, R. A. L.; Cory, R. A. *Europhys. Lett.* **1994**, *27*, 59. (b) Keddie, J. L.; Jones, R. A. L.; Cory, R. A. *Trans. Faraday Discuss.* **1994**, *98*, 219.
- (3) (a) Forrest, J. A.; Dalnoki-Veress, K.; Stevens, J. R.; Dutcher, J. R. *Phys. Rev. Lett.* **1996**, *77*, 2002. (b) Forrest, J. A.; Dalnoki-Veress, K.; Dutcher, J. R. *Phys. Rev. E* **1997**, *56*, 5705. (c) Mattsson, J.; Forrest, J. A.; Borjesson, L. *Phys. Rev. E* **2000**, *62*, 5187.
- (4) (a) Xie, L.; DeMaggio, G. B.; Frieze, W. E.; DeVries, J.; Gilday, D. W.; Hristov, H. A.; Yee, A. F. *Phys. Rev. Lett.* **1996**, *74*, 4947. (b) Tanaka, K.; Taura, A.; Ge, S.; Takahara, A.; Kajiyama, T. *Macromolecules* **1996**, *29*, 3040. (c) Meyers, G. F.; DeKoven, B. M.; Seitz, J. T. *Langmuir* **1992**, *8*, 2330. (d) Hall, D. B.; Hooker, J. C.; Torkelson, J. M. *Macromolecules* **1997**, *30*, 667. (e) Liu, Y.; Russell, T. P.; Samant, M. G.; Stohr, J.; Brown, H. R.; Cossy-Favre, A.; Diaz, J. *Macromolecules* **1997**, *30*, 7768.
- (5) Lazare, S.; Soullignac, J. C.; Fragnaud, P. S. *Appl. Phys. Lett.* **1987**, *50*, 624.
- (6) Aspnes, D. E.; Studna, A. A. *Appl. Opt.* **1975**, *14*, 220.
- (7) (a) Grandqvist, C. G.; Hunderi, O. *Phys. Rev. B* **1977**, *16*, 3513. (b) Aspnes, D. E.; Theeten, J. B.; Hottier, F. *Phys. Rev. B* **1979**, *20*, 3292.
- (8) Mansfield, K. F.; Theodorou, D. N. *Macromolecules* **1991**, *24*, 6283.
- (9) Zangwill, A. In *Physics at Surfaces*; Cambridge University Press: Cambridge, 1992; p 8.
- (10) Weidner, S.; Kuhn, G.; Decker, R.; Roessner, D.; Friedrich, J. *J. Polym. Sci., Part A: Polym. Chem.* **1998**, *36*, 1639.

MA0012797